Chemical Research in Toxicology

Article

pubs.acs.org/crt

Modulation of Cytotoxicity by Transcription-Coupled Nucleotide Excision Repair Is Independent of the Requirement for Bioactivation of Acylfulvene

Claudia Otto,[†] Graciela Spivak,[‡] Claudia M.N. Aloisi,[†] Mirco Menigatti,[§] Hanspeter Naegeli,[∥] Philip C. Hanawalt,[‡] Marina Tanasova,[†,⊥] and Shana J. Sturla*[,†]

[†]Department of Health Sciences and Technology, ETH Zurich, 8092 Zurich, Switzerland

[‡]Department of Biology, Stanford University, Stanford, California 94305, United States

[§]Institute of Molecular Cancer Research, University of Zurich, 8057 Zurich, Switzerland

[∥]Institute of Pharmacology and Toxicology, University of Zurich-Vetsuisse, 8057 Zurich, Switzerland

[⊥]Department of Chemistry, Michigan Technological University, Houghton, Michigan 49932, United States

Supporting Information

ABSTRACT: Bioactivation as well as DNA repair affects the susceptibility of cancer cells to the action of DNA-alkylating chemotherapeutic drugs. However, information is limited with regard to the relative contributions of these processes to the biological outcome of metabolically activated DNA alkylating agents. We evaluated the influence of cellular bioactivation capacity and DNA repair on cytotoxicity of the DNA alkylating agent acylfulvene (AF). We compared the cytotoxicity and RNA synthesis inhibition by AF and its synthetic activated analogue *iso*-M0 in a panel of fibroblast cell lines with deficiencies in transcription-coupled (TC-NER) or global genome nucleotide excision repair (GG-NER). We related these data to the inherent bioactivation capacity of each cell type on the basis of mRNA levels. We demonstrated that specific inactivation of TC-NER by siRNA had the largest positive impact on AF activity in a cancer cell line. These findings establish that transcription-coupled DNA repair reduces cellular sensitivity to AF, independent of the requirement for bioactivation.

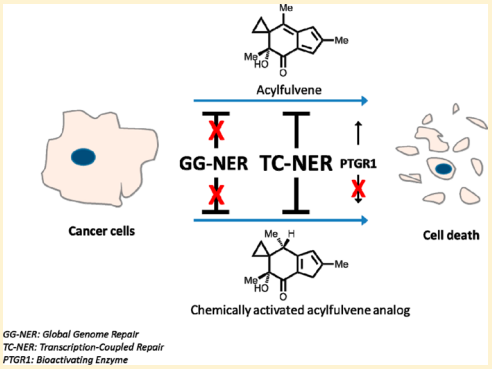

INTRODUCTION

DNA repair contributes significantly to the responses of mammalian cells to DNA-alkylating drugs.[1] In addition, it is well-established that xenobiotic-metabolizing enzymes can strongly influence the cellular responses, either by bioactivation or through detoxification.[2] Reliable interpretation of biological end points requires consideration of possible relationships between these two processes, i.e. repair and metabolism, especially in the context of metabolically activated DNA alkylating agents. For the DNA-alkylating antitumor acylfulvenes (AFs) and their natural product precursor illudin S,[3,4] both DNA repair and bioactivation have been implicated in cytotoxicity; however, their potentially competing influences have not been evaluated. Understanding the relative contributions of repair and metabolism to drug cytotoxicity may lead to more reliable predictions of toxic outcomes and could facilitate the development of more selective chemotherapies. Furthermore, this information may provide predictive markers to aid in selection of patients who may respond more effectively to chemotherapies with DNA alkylating drugs.

The AF class of compounds, which includes the hydroxymethylated analog HMAF, an experimental clinical drug called irofulven (Scheme 1), are DNA-alkylating anticancer agents derived from illudin natural products. AFs have several favorable characteristics for applications in chemotherapy.[5] In cell-based cytotoxicity studies, AFs were shown to induce apoptosis in tumor cells but were cytostatic in normal cells.[6] In tumor xenografts, HMAF was a more effective tumor growth inhibitor than cisplatin, doxorubicin, irinotecan, or mitomycin C, and it also sensitized multidrug-resistant cells to some conventional chemotherapeutic drugs.[7−9] Despite encouraging preclinical data,[4] however, the results from early clinical trials were ambiguous, and a Phase III clinical trial was terminated.[10] Although the clinical outcomes were insufficient for promoting the drug, certain individuals exhibited outstanding results. Thus, there is renewed interest in the clinical potential of acyfulvenes[11] in the context of biomarker-driven personalized medicine strategies, in which patients can be stratified on the basis of molecular markers, such that those who most likely benefit from the therapy may be identified.[12]

Received: July 11, 2016
Published: January 11, 2017

DOI: 10.1021/acs.chemrestox.6b00240
Chem. Res. Toxicol. XXXX, XXX, XXX−XXX

Scheme 1. Enzymatic (Top) or Chemical (Bottom) Reduction of AF Yields Isomeric Reactive Intermediates That Form the Same AF-DNA Adduct

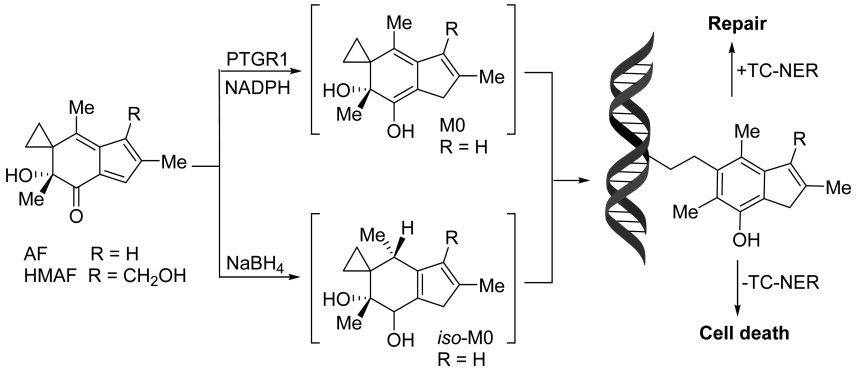

The DNA alkylation and cytotoxicity of AF and HMAF have been shown to depend upon cellular drug-bioactivating capacity, specifically the capacity for enone reduction.[13−17] It has been shown that reductive bioactivation of AF is mediated by NADPH-dependent prostaglandin reductase 1 (PTGR1), also referred to as alkenal/one oxidoreductase (AOR), and that this activity promotes its cytotoxicity.[14,17,18] AF alkylates purine bases through interactions in the minor groove of DNA, leading to depurination and subsequent strand breaks.[16] Increased levels of AF-specific DNA adducts correlate with higher levels of PTGR1.[14,18] Cells that overexpress PTGR1 by 10-fold suffered 4-fold higher levels of AF-induced DNA adducts than control cells. However, adduct levels decreased as a function of the duration of treatment,[18] possibly due to repair.

In addition to the well-established association of AF toxicity with reductive bioactivation, cell resistance to HMAF and illudin S was found to be dependent upon nucleotide excision repair (NER).[19−22] NER can remove a wide variety of mainly bulky DNA lesions such as UV-induced photoproducts and chemical adducts. NER is divided in two subpathways: transcription-coupled NER (TC-NER) removes DNA lesions exclusively from the template strands in actively transcribed DNA,[23,24] whereas global genome NER (GG-NER) repairs lesions throughout the entire genome regardless of transcriptional activity. TC- and GG-NER operate by similar mechanisms, except for the initial damage recognition step. For GG-NER, damage recognition is performed by XPC in complex with hRAD23b and in some cases by XPE (DDB2); TC-NER requires translocating RNA polymerase II as well as the CSB, CSA, and UVSSA proteins but not XPC and XPE.[20] When the cytotoxicity of illudin S and HMAF was evaluated in NER deficient cells, both compounds were more toxic than in normal cells, while deficient base excision repair had no significant effect.[4,20] Interestingly, the cytotoxicity was specifically reduced by effective TC-NER but not impacted by GG-NER.[21]

Although it is well-established that PTGR1-mediated reductive bioactivation enhances AF cytotoxicity, it is not known whether this process may confound the interpretation of AF cytotoxicity data from human fibroblasts with variable repair capacities.[21] Therefore, we evaluated reductive bioactivation in the context of cellular TC-NER-proficiency, employing a combination of strategies. A synthetic analogue of AF that is chemically activated and, therefore, does not require PTGR1 for activation (*iso*-M0, Scheme 1)[17] was tested in fibroblasts with varying NER capacities to determine the relative contributions of bioactivation and DNA repair to the cellular response to AF. *Iso*-M0 is isomeric to the reactive intermediate formed during PTGR1-mediated activation, and it alkylates DNA to yield the same DNA adduct profile as AF in the presence of PTGR1. However, the potency of *iso*-M0 is independent of cellular reductive bioactivation capacity.[17] We compared cytotoxicity and RNA synthesis inhibition induced by AF, HMAF, and *iso*-M0 in human fibroblasts that were proficient or deficient in GG-NER, TC-NER, or both. Levels of the bioactivating enzyme PTGR1 were also compared among these human fibroblast strains. Furthermore, to compare the AF sensitivity of cells with modulated bioactivation and repair capacity but an otherwise isogenic background, SW480 cells and SW480 cells engineered to overexpress the AF-bioactivating enzyme PTGR1 (SW480-PTGR1) were treated with siRNA for selected NER factors, and modulation of cytotoxicity was evaluated.

MATERIALS AND METHODS

Cell Strains and Culture Conditions. Primary fibroblast cell lines were purchased from Coriell Institute for Medical Research. WT GM00037 are nonfetal primary fibroblasts from a repair proficient donor. XP and CS cells are from unexposed skin biopsies of patients with xeroderma pigmentosum (XP) or Cockayne syndrome (CS). SW-480 cells were provided by Dr. Giancarlo Marra (University of Zurich). SW-480-PTGR1 cells were generated as described by Pietsch et al.[18]Fibroblasts were maintained as monolayers in 75 cm^2 flasks in GIBCO minimum essential medium with Earle's salts and glutamax, supplemented with 15% FBS and 1% penicillin−streptomycin in a humidified, 5% CO_2 atmosphere at 37 °C. SW-480 control cells and SW-480 cells stably transfected to overexpress PTGR1 were maintained in RPMI 1640 medium with 10% fetal calf serum (v/v) and 1% pen/strep (v/v) and incubated at 37 °C in a humidified incubator containing 5% CO_2.

Chemicals. (−)-Illudin S, isolated from *Omphalotus* species,[25] was provided by MGI Pharma (Bloomington, MN). (−)-Acylfulvene ((−)-AF) was synthesized from illudin S by a previously published procedure.[5] The chemically activated AF analogue (*iso*-M0) was synthesized from AF following a previously published procedure.[17] 3-[4, 5-Dimethyl-2-yl]-2,5-diphenyltetrazolium bromide (MTT) was from SIGMA. Stock 100× solutions in DMSO were stored at −20 °C.

Cytotoxicity Assay. Cells were plated in 96-well plates (~2×10^3 per well) and treated with solutions of test compounds that were diluted with culture medium (0.1% final concentration of DMSO). DMSO-treated cells were used as control, and backgrounds from cell-free wells were subtracted. After 1 h, cells were washed, and the medium was replaced with fresh drug-free medium and further incubated for 72 h. Cell survival was measured by adding 50 μL of medium containing 0.5 mg/mL MTT per well and incubating for 4 h at 37 °C; the intensity of the developed color was assessed by monitoring absorbance at 540 nm. Each data set was acquired in

DOI: 10.1021/acs.chemrestox.6b00240
Chem. Res. Toxicol. XXXX, XXX, XXX−XXX

triplicate for each of 3 or more experiments, and the averaged absorption values of the drug-treated cells were normalized to those of DMSO-treated cells (assigned as 100% viability). Treated cells were examined microscopically to confirm cytotoxicity at the highest doses used.

RNA Synthesis Recovery. RNA synthesis levels in AF- and *iso*-M0-treated cells were determined by measuring incorporation of radiolabeled uridine into RNA as a function of postincubation period. Fibroblasts were grown in 75 cm^2 flasks with complete medium containing 0.02 μCi [2-^{14}C]thymidine (Moravek) until semiconfluency (2−3 days). Cells were then transferred to 12-well plates, as follows: the [2-^{14}C] thymidine-containing medium was collected, cells were treated with 2 mL of 0.25% trypsin-EDTA at 37 °C for 5 min and transferred to centrifuge tubes. Cells were then pelleted by centrifugation (5 min, 5000*g*), resuspended in the collected [2-^{14}C] thymidine-containing medium, plated in 12-well plates, and incubated overnight. Two 12-well plates were set up for each cell line, with 3 wells for each treatment and incubation time. For drug treatments, the [2-^{14}C] thymidine-containing medium was collected, the wells rinsed with PBS, and 0.5 mL of HBSS containing AF (20 ng/mL), *iso*-M0 (20 ng/mL), or no drug (control) was added to each well. After 1 h of incubation at room temperature, the drug was removed, and 0.5 mL of the reserved [2-^{14}C] thymidine-containing medium was added to each well. The "24 h" plates were immediately placed in the incubator.

To pulse-label nascent RNA, 0.1 mL of medium containing [5-^{3}H]uridine (Moravek) was added to each well to achieve a 3 μCi/ml final concentration. The cells were incubated for 1 h at 37 °C, the medium removed, and the wells were rinsed twice with PBS. Lysis solution (0.5 mL; 150 mM NaCl, 10 mM Tris HCl at pH 8.0, 1 mM EDTA, 0.5% SDS, and 10 mg/mL proteinase K) was added to each well. The plates were incubated at 37 °C for 1 h, the lysates were transferred to centrifuge tubes, the wells were rinsed with 0.5 mL of PBS, and rinses were added to the corresponding samples. Lysates were incubated at 54 °C for 1 h. Trichloroacetic acid (20%, 0.5 mL) was added to each tube, and samples were chilled at 4 °C for at least 2 h. Precipitated nucleic acids were collected on Millipore HA 0.45 μm filters, which were dried under a heat lamp. Radioactivity was measured by scintillation counting. Three biological experiments were done, each in triplicate. Samples labeled with only ^{14}C or ^{3}H were used to calculate and correct overlaps. Ratios of ^{3}H to ^{14}C radioactivity were used to normalize the amount of transcription to the number of cells and were averaged for each set of triplicate measurements. Recoveries were calculated relative to the ratios in untreated cells.

Reverse-Transcription Real Time PCR Analysis of PTGR1 Expression. Untreated cells were collected from two flasks at 90−95% confluence as follows: 2 mL of 0.25% trypsin-EDTA was added, and the cells were incubated for 5 min at 37 °C. Total mRNA was extracted using the QIAGEN miRNeasy mini kit and kept on dry ice until cDNA synthesis (see Supporting Information for primer sequences and PCR conditions). Synthesis of first-strand cDNA was performed with the Transcriptor First Strand cDNA Synthesis kit (Roche) according to manufacturer's instructions with random hexamer primers. Expression of prostaglandin reductase 1 (PTGR1, Gene ID: 22949) and of the reference gene porphobilinogen deaminase (PBGD, Gene ID: 3145) was measured with the LightCycler 480 real-time PCR system and a LightCycler 480 SYBR Green I master kit (Roche). The analysis was performed in duplicate, and relative PTGR1 expression in the different cell lines was calculated by the method of Pfaffl et al.[26]

siRNA of NER Factors in SW480 and PTGR1-Overexpressing Cells. SW-480 cells were maintained in RPMI 1640 medium with 10% fetal calf serum (v/v) and 1% pen/strep (v/v) and incubated at 37 °C in a humidified incubator containing 5% CO_2. siRNA sequences (Table S2, Supporting Information) were purchased from Microsynth. Transfections were performed with Lipofectamine RNAiMAX according to the manufacturer's protocol (Invitrogen). The siRNA concentrations were 10 nM for noncoding siRNA and the silencing of XPA, XPC, and CSB targets (siRNA sequences are listed in Supporting Information). Protein levels were analyzed 72 h after siRNA transfections by Western blot. For treatment with Acylfulvene, cells were seeded 48 h after siRNA transfection in 96-well plates at a density of 3.0×10^3 cells/well and were allowed to attach overnight. Cell viability experiments were initiated by replacing the maintenance media with media containing AF (0, 10, 100, 150, 300, 500, 1000, and 5000 nM final concentration, 0.1−0.5% DMSO). Cell viability was measured 48 h later with the CellTiter-Glo luminescent cell viability assay according to the manufacturer's protocol (Promega). With this assay, the number of viable cells in culture is determined on the basis of ATP quantification as an indicator of metabolically active cells. Three independent experiments were performed, and each condition was analyzed three times (i.e., three biological replicates, each with three technical replicates). Reduction of protein expression was confirmed by Western blot analysis whereby after 72 h of siRNA treatment, cells were lysed in RIPA buffer (Pierce, Thermo Scientific) containing protease inhibitors (Complete Tablets EDTA-free EASY-pack, Roche). Protein samples (40 μg) were loaded onto an SDS−PAGE gel (4−12% NuPAGE bis-tris gels, Invitrogen), electrophoresed at 200 V for 180 min in 1XMOPS running buffer (NuPAGE MOPS SDS Running buffer 20×, Life techonologies) and transferred onto PVDF membranes (Amersham Hybond-P) at 30 V for 50 min. Staining was performed with the following primary antibodies and respective secondary HRP antibodies: Mouse-anti-XPC (Abcam, 1:500) and rabbit-anti-CSB (Abcam, 1:500). All primary antibodies were diluted in 3% BSA, TBS-Tween. Western blots were developed with Pierce ECL Western blotting substrate (Thermo Scientific) and exposured to X-ray film.

RESULTS

Cytotoxicity of AF and *iso*-M0 in Human Fibroblasts with Different DNA Repair Proficiencies. In previous studies, CSB deficiency in human fibroblasts, associated with a lack of TC-NER function, was shown to correlate with higher toxicity of illudin S and HMAF.[20,21] In contrast, XPC deficiency, associated with a lack of GG-NER function but proficiency in TC-NER, had no impact on HMAF or illudin S cytotoxicity,[20,21] indicating that HMAF- and illudin S-induced DNA adducts are selectively processed by TC-NER. However, in those studies, AF was not tested, and the bioactivation potential of the cells was not measured. Therefore, to first confirm that TC-NER proficiency influences AF cytotoxicity in the same manner as that for HMAF and illudin S, we evaluated the toxicity of AF in human fibroblast cells competent for GG- and/or TC-NER, or neither. As anticipated, AF was most active in NER-deficient XPA cells, inducing 70% cell death at 2 ng/mL (Figure 1A). Somewhat lower cytotoxicity (60% cell death) was detected in TC-NER-deficient CSB cells. The GG-NER-deficient XPC and NER-proficient WT cells were resistant to low AF concentrations (1−5 ng/mL) but responded with 20% and 40% lethality, respectively, at higher AF concentration. The higher susceptibility of XPA and CSB cells ($p < 0.039$) implicates NER (and specifically TC-NER) as a factor controlling AF cytotoxicity. Furthermore, AF cytotoxicity was enhanced specifically when TC-NER was compromised. As anticipated, these data for AF are consistent with those previously reported for HMAF and illudin S.[20,21]

After confirming that AF cytotoxicity was enhanced in XPA or CSB cells, we evaluated the survival of the same cells treated with the AF analogue *iso*-M0, in order to control for any possible alteration of this profile due to potential differences in cellular bioactivating capacity (Figure 1B). We found that NER-deficient XP-A and TC-NER deficient CS-B cells were significantly susceptible to *iso*-M0, while WT and GG-NER-deficient XP-C cells were resistant. Thus, AF and *iso*-M0 elicited similar responses in XP cells, with TC-NER-deficient

DOI: 10.1021/acs.chemrestox.6b00240
Chem. Res. Toxicol. XXXX, XXX, XXX−XXX

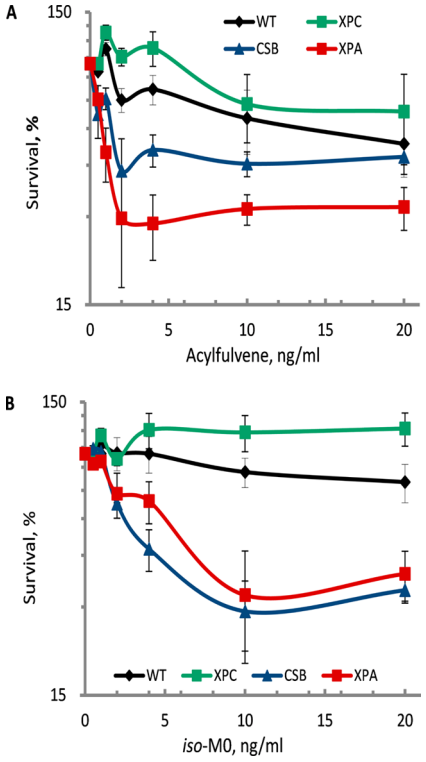

Figure 1. Cytotoxicities of AF and *iso*-M0 in human fibroblast cells. Cells were exposed to AF (A) or *iso*-M0 (B) for 1 h, followed by 72 h postincubation in drug-free medium and assayed for cell survival.

cells being susceptible and TC-NER-proficient cells being resistant toward AF or *iso*-M0.

AF and Its Activated Analogue (*iso*-M0) Inhibit RNA Synthesis. Reduction in cellular transcriptional level in response to a DNA damaging agent reflects the proficiency of the cells in TC-NER because of the link between DNA damage-induced arrest of RNA polymerase II and initiation of TC-NER.[24,27] We analyzed the propensity of AF and *iso*-M0 to inhibit RNA synthesis during 1-h treatments with the drugs and monitored its recovery in WT, XP, and CS cells. Nascent RNA levels were measured both immediately after treatment with AF or *iso*-M0 (0 h) or following 24 h postincubation of the treated cells in drug-free medium (24 h). Data immediately after treatment were collected to assess inhibitory activities of AF and *iso*-M0, while the changes in RNA levels after 24 h of postincubation should reflect the potential of the cells to recover from the damage, thus providing a measure of TC-NER or GG-NER involvement in AF and *iso*-M0 induced lesion recognition and repair.

Immediately after AF treatment, RNA synthesis was inhibited in all cell lines, although to different extents (Figure 2; AF): by 80% in WT, by 65% in CSB cells, and by 55% ($p < 0.039$) in XP-A or XP-C cells. Treating cells with *iso*-M0 resulted in relatively similar levels of RNA synthesis inhibition, ranging within 47−55% (Figure 2, *iso*-M0).

After 24 h postincubation in drug-free medium, cells proficient in TC-NER almost completely recovered from the drug-induced damage (Figure 2; AF, 24 h and *iso*-M0, 24 h). Recovery was 74% and 87% in AF-treated WT and XPC cells, respectively, and complete in *iso*-M0-treated WT and XPC cells. In contrast, RNA synthesis did not recover in drug-treated NER-deficient XPA or TC-NER-deficient CSB cells. Although AF completely suppressed RNA synthesis in TC-NER-deficient

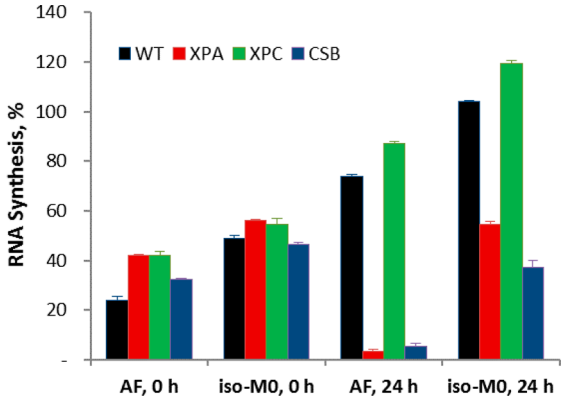

Figure 2. RNA levels in cells treated with 20 ng/mL AF or *iso*-M0 immediatly after 1 h of treatment (AF, 0 h, and *iso*-M0, 0 h) and after 24 h postincubation in drug free medium (AF, 24 h, and *iso*-M0, 24 h). Values were normalized to those in mock-treated cells.

cells 24 h after treatment, *iso*-M0 had no further inhibitory effect on RNA synthesis in XPA and CSB cells during postincubation (Figure 2, AF, 24 h and *iso*-M0, 24 h).

PTGR1 Levels in WT, XP, and CSB Cells. AF cytotoxicity and levels of AF-specific DNA adducts have been shown to correlate with the abundance of PTGR1 in cell-based and cell-free systems; the mechanism of cellular bioactivation involves reduction of the unsaturated enone by this NADPH-dependent reductase.[13−17,28] We examined basal PTGR1 levels in cell lysates of WT, XPA, XPC, and CSB cells by real time RT-PCR analysis. The WT fibroblasts expressed PTGR1 the least. In XPA and XPC cells, the average levels of PTGR1 mRNA appeared to be 2.5-fold higher than in WT cells, and in CSB cells, 1.8-fold higher (Figure S1, Supporting Information). These data suggest that the differences observed for the susceptibility of the fibroblasts to AF (Figure 1) do not correlate with bioactivation potential. Moreover, PTGR1 levels may be slightly lower in CSB than XPA cells, yet the CSB cells are more sensitive, substantiating the overriding importance of DNA repair differences in the response to the drug.

Transient Depletion of Certain NER Factors in Cells Can Enhance AF Cytotoxicity. To compare AF sensitivity in cells with modulated bioactivation and repair capacity but an otherwise isogenic background, SW480 human cancer cells engineered to overexpress the AF-bioactivating enzyme PTGR1 (SW480-PTGR1)[18] were treated with siRNA for XPC and CSB, and the impact on cytotoxicity was evaluated. Cells were transfected with siRNA for down regulation of XPC or CSB separately (Table S2, Supporting Information). Transfected cells were reseeded 48 h later, and cellular sensitivity toward AF was evaluated after another 48 h period; XPC and CSB knock-down was confirmed to be effective by Western blot (Figure S2, Supporting Information). The SW480-PTGR1 cells, which had 17-fold higher levels of PTGR1 protein,[18] were more sensitive to the drug as compared to control cells. For nontargeted control transfections, EC_{50} values were 141 nM in SW480-PTGR1 cells vs 255 nM in SW480 cells (Figure 3). These results are consistent with a previous report in which significant increases in DNA adduct levels and cytotoxicity were detected in SW480-PTGR1 vs SW480 cells.[18]

For both cell lines SW480 and SW480-PTGR1, significantly higher sensitivity toward AF was observed when CSB was transiently silenced: the EC_{50} went from 255 nM (control) to 29 nM (CSB) in SW480 cells and from 141 nM (control) to 66

DOI: 10.1021/acs.chemrestox.6b00240
Chem. Res. Toxicol. XXXX, XXX, XXX−XXX

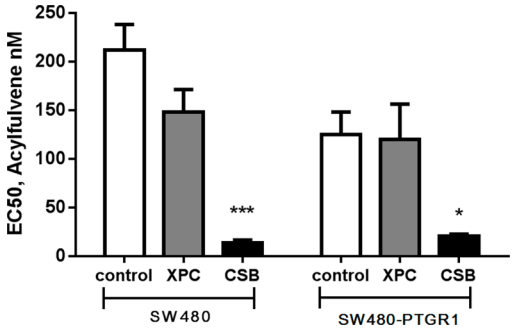

Figure 3. Cytotoxicity of AF in SW480 wild type (SW480) and PTGR1-overexpressing cells (SW480-PTGR1) transfected with siRNA to knock-down GG-NER (XPC) or TC-NER (CSB). Control cells were transfected with a noncoding sequence of siRNA (control). Cell viability was measured with two technical replicates from each of three independent experiments. Mean values and standard errors of the mean are indicated. Statistical significance of differences relative to the control was calculated using two-way ANOVA with a Dunnett post hoc test (*P < 0.05, **P < 0.01, and ***P < 0.001).

nM (CSB) in SW480-PTGR1 (Figure 3). Furthermore, silencing XPC had no significant impact on toxicity relative to the noncoding controls. These data further corroborate the conclusion from experiments in primary fibroblasts, with a significant increase in susceptibility to the drug demonstrated when CSB but not XPC was silenced, confirming the role of TC-NER in AF repair.

DISCUSSION

The experimental anticancer drug HMAF is not toxic to TC-NER-proficient cells,[19,20] whereas cells with high capacity for enone reduction are particularly susceptible to the drug.[13−17,28] Following activation by enone reduction, acylfulvene alkylates DNA primarily from minor-groove binding and modification of the 3-position of Adn. Roles for DNA repair and drug bioactivation in the cytotoxicity of AFs have been independently studied, but the potentially confounding interplay between these factors has not been addressed in concert.

Using human fibroblasts deficient in TC-NER activity (CSB), GG-NER activity (XPC), both repair pathways (XPA), or neither (WT), we found that AF was most potent toward XPA and CSB cells. These cellular response patterns are very similar to those that were previously reported for the AF analogue HMAF by Koeppel[21] and Jaspers.[20] We also determined that the synthetic analogue *iso*-M0, which does not require bioactivation, elicits toxic responses in cells with defective TC-NER. In addition to the assessment of cell sensitivity, we evaluated the recovery of RNA synthesis in cells immediately following treatment with AF and after a 24 h recovery period; this assay reveals the ability of the cells to remove lesions from transcribed DNA strands. Furthermore, we characterized mRNA levels of the AF-bioactivating enzyme PTGR1 in the fibroblast strains. Considering the results of these three studies together, a picture that emerges is that despite slightly lower PTGR1 in CSB cells, cell viability is decreased and cells fail to recover RNA synthesis capacity (Table 1). These data for AF and those of Koeppel et al.[21] and Jaspers et al.[20] reported previously for HMAF support the concept that cellular resistance to AFs is governed by TC-NER proficiency.

The relative impacts of bioactivation and repair were further established by a chemical probe approach using *iso*-M0, a

Table 1. Relative Direction and Magnitude of Changes in Bioactivation Protein Levels, Cell Survival, and Recovery of RNA Synthesis

	Relative to response of WT fibroblasts [a]		
	XPA	XPC	CSB
PTGR1-associated mRNA levels	↑↑	↑↑	↑
Cell survival [b]	↓	↔	↓
Recovery of RNA Synthesis [c]	↓	↔	↓

[a]Red arrows pointing up indicate increased levels relative to WT; green arrows pointing down indicate decreased response relative to WT; orange horizontal arrows indicate lack of effect. The number of red arrows reflects magnitude of increase. [b]2 h treatment, 20 ng/mL AF, and 72 h regrowth. [c]1 h treatment, 20 ng/mL AF, and 24 h regrowth.

synthetic analogue of AF that does not require bioactivation to alkylate DNA in the same manner as AF.[18] Thus, *iso*-M0 was equally cytotoxic to XPA and CSB cells, whereas AF cytotoxicity differed, possibly due to the slightly higher levels of PTGR1 in the XPA cells. These data are consistent with previous findings that increased bioactivation activity increases levels of DNA modification and the cytotoxic response in NER-deficient cells.[13−17,28] Moreover, this process does not appear to detract from the importance of TC-NER in cellular resistance to AF or its bioactive forms. Interestingly, the CSB cells seem to be more sensitive to *iso*-M0 than to AF at higher doses (20 ng/mL, Figure 1), yet RNA synthesis recovery in the same cells was greater for *iso*-M0 than AF (Figure 2). The reason for this observation could be a more promiscuous reactivity of *iso*-M0, modifying a wider range of biomolecules also contributing to cytotoxicity but reducing the contribution of the impedance of RNA synthesis.

While acylfulvene DNA adducts are quite unstable in naked DNA, with a depurination half-life of around 2−8 h, they appear to persist longer in a human cell line, where their half-life is around 1 d.[16,22,28] When those cells were treated with a G2 checkpoint inhibitor that reduces cellular DNA repair function, their persistence was extended, and the half-life was 12 d.[22] Taken together with the results presented here, the model that emerges is that AF adducts persist long enough and are sufficiently large to stall RNA Pol II; however, it appears that they orient in the duplex such that they are non-helix-distorting and thus are not recognized by XPC. This repair susceptibility profile is similar to that of aristolochic acid (AA); however, unlike acylfulvene adducts, AA-derived aristolactam adducts are non-depurinating.[29−31] A mechanistic and structural basis for the lack of repair of AA-adducts by GG-NER is that AA-adducts cause only minor destabilization of the DNA duplex and intercalate in the helix, avoiding recognition by the XPC-HR23B complex of the GG-NER pathway to initiate repair.[32] Likewise, acetylaminoflourine modifies the C8- and N2-positions of purines, and the 3-(deoxyguanosin-N2-yl)-2-acetylaminofluorene adduct (dG(N2)-AAF) but not *N*-

DOI: 10.1021/acs.chemrestox.6b00240
Chem. Res. Toxicol. XXXX, XXX, XXX−XXX

(deoxyguanosin-8-yl)-2-acetylaminofluorene (dG(C8)-AAF) requires TC-NER for removal.[33] These results are consistent with the lack of removal of dG(N2)-AAF in animals administered acetylaminoflourene[34] and the detailed characterization of the structure of the adduct where the modification is well accommodated in the minor groove with minimal solvent exposure.[35]

Indeed, the capacity for certain bulky DNA adducts to evade GG-NER is well documented in the literature, and in these cases, inefficient removal is posited to contribute to mutagenic potential. The thermally stable formamidopyrimidine adduct derived from decomposition of the initially formed aflatoxin adduct forms an intercalated structure that is not repaired.[36,37] Nitrochrysene gives rise to a C8-Adn adduct that is resistant to repair in vitro, whereas for animals exposed to the heterocyclic amine 2-amino-3-methylimidazo[4,5-*f*]quinolone (IQ), in analogy to AAF observations, it is dG-N2-IQ that is recalcitrant to repair compared to dG-C8-IQ.[38,39] Polycyclic aromatic hydrocarbons, such as dibenzo[*a*,*l*]pyrene, benzo[*g*]chrysene, benzo[*c*]phenanthrene, and 3-nitrobenzanthrone form adducts that are generally resistant to repair, and data available suggest the adducts have non-distorting intercalation-type conformations that maintain normal Watson−Crick base pairing capacity.[40−43] In these cases, the capacity of TC-NER to process the corresponding adducts was not established, and the GG-NER-recalcitrant adducts are sometimes minor DNA alkylation products. Nonetheless, by analogy, it may be anticipated that these bulky adducts previously characterized to be GG-NER resistant could be susceptible to selective repair by TC-NER and that, moreover, the GG-NER resistance of the AF adduct may contribute to mutagenesis.[44]

Silencing NER factors in the human colon cancer cell line SW480 with standard or elevated PTGR1 levels in SW480 cells stably transfected with Myc-DDK tagged PTGR1 cDNA[18] corroborated that also in a cancer cell line, TC-NER has a significant influence on AF toxicity independent of bioactivation and, moreover, supports beyond a doubt that the differences in repair-deficient fibroblasts are not due to inherent differences between the individuals from whom cells were obtained (Figure 3). Silencing CSB by siRNA led to a 2−9-fold increase in toxicity, a change with a magnitude similar to what was observed previously (2−4 fold increase) when the same experiment was performed with cisplatin in a different cancer cell line.[45] Furthermore, the association between AF cytotoxicity and PTGR1 expression observed here and previously[13−17,28] is consistent with the positive correlation between HMAF cytotoxicity and enone reduction capacity characterized previously in a panel of 60 human cancer cell lines, where DNA repair proficiency differences were not considered.[13] In light of the current results, this correlation should be further considered by also integrating knowledge of the DNA repair proficiencies in those cells. For example, leukemia-derived HL-60 cells are TC-NER proficient[46] and were relatively insensitive to HMAF. In contrast, ovarian and prostate cancer cells are TC-NER-deficient[45,47] and were 100-fold more susceptible to HMAF.[13] It should be noted, however, that ovarian and prostate cancer cells have 10-fold higher enone reductase capacity than leukemia cells[13] and that enhanced bioactivating capacity, in addition to TC-NER-deficiency, could contribute to the strong activity of HMAF in these cells. Finally, TC-NER-proficient breast cancer cells (MCF7 and MBA-MB-231) were 10-fold more resistant than ovarian and prostate cancers to HMAF, despite being equally efficient in enone-reduction.[13] These relationships suggest that for bioactivated DNA alkylating drugs, establishing both bioactivation capacity and pathway-specific repair proficiency of tumors may be an effective combination of biomarkers for predicting outcome of chemotherapy.

CONCLUSION

We established that TC-NER proficiency significantly reduces AF cytotoxicity in a human cancer cell line and in primary fibroblasts. These data corroborate the role of repair while also considering potential bioactivation influences, demonstrating a chemistry-based approach (i.e., chemically activated drug analogue) for dissecting the role of bioactivation from other biochemical factors influencing drug activity. These results imply that the major AF-DNA adduct, while bulky enough to impede transcription, can be well-accommodated in the DNA duplex. This study suggests that future development of AF-related clinical candidates should account for DNA repair and bioactivation-related biomarkers, as well as a possible role for combined therapeutic strategies involving the inhibition of TC-NER.

ASSOCIATED CONTENT

Supporting Information

The Supporting Information is available free of charge on the ACS Publications website at DOI: 10.1021/acs.chemrestox.6b00240.

Relative PTGR1 levels as determined by real time reverse transcription PCR; gene sequences for the real time PCR analysis; silencing of NER factors XPC and CSB in SW480 and SW480-PTGR1 cells (Western blots); and corresponding siRNA sequences (PDF)

AUTHOR INFORMATION

Corresponding Author

*Department of Health Sciences and Technology, Institute of Food, Nutrition and Health, ETH Zurich, Schmelzbergstrasse 9, Zurich 8092, Switzerland. E-mail: sturlas@ethz.ch.

ORCID

Shana J. Sturla: 0000-0001-6808-5950

Funding

We acknowledge support from the Susan G. Komen for the Cure foundation (M.T.), National Cancer Institute (CA123007 and CA077712), National Institutes of Environmental Health Sciences (ES018834), European Research Council (260341), and the Swiss National Science Foundation (156280).

Notes

The authors declare no competing financial interest.

ACKNOWLEDGMENTS

We acknowledge Sabine Senger for technical assistance with cell culture.

ABBREVIATIONS

NER, nucleotide excision repair; TC-NER, transcription-coupled NER; GG-NER, global genome NER; PTGR1, prostaglandin reductase 1; AF, acylfulvene; HMAF, hydroxymethylacylfulvene; DMSO, dimethyl sulfoxide; WT, wild type; XP, xeroderma pigmentosum; CS, cockayne syndrome

DOI: 10.1021/acs.chemrestox.6b00240
Chem. Res. Toxicol. XXXX, XXX, XXX−XXX

REFERENCES

(1) (2011) *DNA Repair in Cancer Therapy: Molecular Targets and Clinical Applications*, Kelley, M. R., Ed. Elsevier, London, San Diego.

(2) Ripp, S. L. (2008) *Advances in Bioactivation Research*, Springer, New York.

(3) Kelner, M. J., McMorris, T. C., Estes, L., Starr, R. J., Rutherford, M., Montoya, M., Samson, K. M., and Taetle, R. (1995) Efficacy of Acylfulvene Illudin analogues against a metastatic lung carcinoma MV522 xenograft nonresponsive to traditional anticancer agents: retention of activity against various mdr phenotypes and unusual cytotoxicity against ERCC2 and ERCC3 DNA helicase-deficient cells. *Cancer Res. 55*, 4936−4940.

(4) Tanasova, M., and Sturla, S. J. (2012) Chemistry and Biology of Acylfulvenes: Sesquiterpene-Derived Antitumor Agents. *Chem. Rev. 112*, 3578−3610.

(5) McMorris, T. C., Kelner, M. J., Wang, W., Diaz, M. A., Estes, L. A., and Taetle, R. (1996) Acylfulvenes, a new class of potent antitumor agents. *Experientia 52*, 75−80.

(6) Woynarowska, B. A., Woynarowski, J. M., Herzig, M. C., Roberts, K., Higdon, A. L., and MacDonald, J. R. (2000) Differential cytotoxicity and induction of apoptosis in tumor and normal cells by hydroxymethylacylfulvene (HMAF). *Biochem. Pharmacol. 59*, 1217−1226.

(7) Sato, Y., Kashimoto, S., MacDonald, J. R., and Nakano, K. (2001) In vivo antitumour efficacy of MGI-114 (6-hydroxymethylacylfulvene, HMAF) in various human tumour xenograft models including several lung and gastric tumours. *Eur. J. Cancer 37*, 1419−1428.

(8) Woo, M. H., Peterson, J. K., Billups, C., Liang, H., Bjornsti, M. A., and Houghton, P. J. (2005) Enhanced antitumor activity of irofulven in combination with irinotecan in pediatric solid tumor xenograft models. *Cancer Chemother. Pharmacol. 55*, 411−419.

(9) Serova, M., Calvo, F., Lokiec, F., Koeppel, F., Poindessous, V., Larsen, A. K., Van Laar, E. S., Waters, S. J., Cvitkovic, E., and Raymond, E. (2006) Characterizations of irofulven cytotoxicity in combination with cisplatin and oxaliplatin in human colon, breast, and ovarian cancer cells. *Cancer Chemother. Pharmacol. 57*, 491−499.

(10) MGI PHARMA, Inc. (2002) MGI PHARMA Stops Phase 3 Irofulven Clinical Trial for Refractory Pancreatic Cancer Patients, in *MGI Pharma press release*, Minneapolis.

(11) Medical Prognosis Institute (2015) MPI's drug Development Arm Oncology Venture and Lantern Pharma Announce Partnership to Advance Irofulven for Metastatic Prostate Cancer, *Company Announcement No. 39*, Hoersholm, DK.

(12) Beckman, R. A., and Chen, C. (2015) Efficient, Adaptive Clinical Validation of Predictive Biomarkers in Cancer Therapeutic Development. *Adv. Exp. Med. Biol. 867*, 81−90.

(13) Dick, R. A., Yu, X., and Kensler, T. W. (2004) NADPH alkenal/one oxidoreductase activity determines sensitivity of cancer cells to the chemotherapeutic alkylating agent irofulven. *Clin. Cancer Res. 10*, 1492−1499.

(14) Neels, J. F., Gong, J., Yu, X., and Sturla, S. J. (2007) Quantitative correlation of drug bioactivation and deoxyadenosine alkylation by acylfulvene. *Chem. Res. Toxicol. 20*, 1513−1519.

(15) Gong, J., Neels, J. F., Yu, X., Kensler, T. W., Peterson, L. A., and Sturla, S. J. (2006) Investigating the role of stereochemistry in the activity of anticancer acylfulvenes: synthesis, reductase-mediated bioactivation, and cellular toxicity. *J. Med. Chem. 49*, 2593−2599.

(16) Gong, J., Vaidyanathan, V. G., Yu, X., Kensler, T. W., Peterson, L. A., and Sturla, S. J. (2007) Depurinating acylfulvene-DNA adducts: characterizing cellular chemical reactions of a selective antitumor agent. *J. Am. Chem. Soc. 129*, 2101−2111.

(17) Pietsch, K. E., Neels, J. F., Yu, X., Gong, J., and Sturla, S. J. (2011) Chemical and enzymatic reductive activation of acylfulvene to isomeric cytotoxic reactive intermediates. *Chem. Res. Toxicol. 24*, 2044−2054.

(18) Pietsch, K. E., van Midwoud, P. M., Villalta, P. W., and Sturla, S. J. (2013) Quantification of acylfulvene- and illudin S-DNA adducts in cells with variable bioactivation capacities. *Chem. Res. Toxicol. 26*, 146−155.

(19) Escargueil, A. E., Poindessous, V., Soares, D. G., Sarasin, A., Cook, P. R., and Larsen, A. K. (2008) Influence of irofulven, a transcription-coupled repair-specific antitumor agent, on RNA polymerase activity, stability and dynamics in living mammalian cells. *J. Cell Sci. 121*, 1275−1283.

(20) Jaspers, N. G., Raams, A., Kelner, M. J., Ng, J. M., Yamashita, Y. M., Takeda, S., McMorris, T. C., and Hoeijmakers, J. H. (2002) Anti-tumour compounds illudin S and Irofulven induce DNA lesions ignored by global repair and exclusively processed by transcription- and replication-coupled repair pathways. *DNA Repair 1*, 1027−1038.

(21) Koeppel, F., Poindessous, V., Lazar, V., Raymond, E., Sarasin, A., and Larsen, A. K. (2004) Irofulven cytotoxicity depends on transcription-coupled nucleotide excision repair and is correlated with XPG expression in solid tumor cells. *Clin. Cancer Res. 10*, 5604−5613.

(22) van Midwoud, P. M., and Sturla, S. J. (2013) Improved efficacy of acylfulvene in colon cancer cells when combined with a nuclear excision repair inhibitor. *Chem. Res. Toxicol. 26*, 1674−1682.

(23) Svejstrup, J. Q. (2002) Mechanisms of transcription-coupled DNA repair. *Nat. Rev. Mol. Cell Biol. 3*, 21−29.

(24) Hanawalt, P. C., and Spivak, G. (2008) Transcription-coupled DNA repair: two decades of progress and surprises, Nature reviews. *Nat. Rev. Mol. Cell Biol. 9*, 958−970.

(25) McCloud, T. G., Klueh, P. A., Pearl, K. C., Cartner, L. K., Muschik, G. M., and Poole, K. K. (1996) Isolation of illudin S from the mature basidiocarp of Omphalotus illudens, and isolation of illudins S and M from the fermentation broth of Omphalotus olearis. *Nat. Prod. Lett. 9*, 87−95.

(26) Pfaffl, M. W. (2001) A new mathematical model for relative quantification in real-time RT-PCR. *Nucleic Acids Res. 29*, e45.

(27) Spivak, G., and Hanawalt, P. C. (2006) Host cell reactivation of plasmids containing oxidative DNA lesions is defective in Cockayne syndrome but normal in UV-sensitive syndrome fibroblasts. *DNA Repair 5*, 13−22.

(28) Pietsch, K. E., van Midwoud, P. M., Villalta, P. W., and Sturla, S. J. (2013) Quantification of acylfulvene- and illudin S-DNA adducts in cells with variable bioactivation capacities. *Chem. Res. Toxicol. 26*, 146.

(29) Sidorenko, V. S., Yeo, J. E., Bonala, R. R., Johnson, F., Scharer, O. D., and Grollman, A. P. (2012) Lack of recognition by global-genome nucleotide excision repair accounts for the high mutagenicity and persistence of aristolactam-DNA adducts. *Nucleic Acids Res. 40*, 2494−2505.

(30) Kucab, J. E., Phillips, D. H., and Arlt, V. M. (2010) Linking environmental carcinogen exposure to TP53 mutations in human tumours using the human TP53 knock-in (Hupki) mouse model. *FEBS J. 277*, 2567−2583.

(31) Rosenquist, T. A., and Grollman, A. P. (2016) Mutational signature of aristolochic acid: Clue to the recognition of a global disease. *DNA Repair 44*, 205−211.

(32) Lukin, M., Zaliznyak, T., Attaluri, S., Johnson, F., and de Los Santos, C. (2012) Solution structure of duplex DNA containing a beta-carba-Fapy-dG lesion. *Chem. Res. Toxicol. 25*, 2423−2431.

(33) Kitsera, N., Gasteiger, K., Lühnsdorf, B., Allgayer, J., Epe, B., Carell, T., and Khobta, A. (2014) Cockayne Syndrome: Varied Requirement of Transcription-Coupled Nucleotide Excision Repair for the Removal of Three Structurally Different Adducts from Transcribed DNA. *PLoS One 9*, e94405.

(34) Culp, S. J., Poirier, M. C., and Beland, F. A. (1993) Biphasic removal of DNA adducts in a repetitive DNA sequence after dietary administration of 2-acetylaminofluorene. *Environ. Health Perspectives 99*, 273−275.

(35) Zaliznyak, T., Bonala, R., Johnson, F., and de Los Santos, C. (2006) Structure and stability of duplex DNA containing the 3-(deoxyguanosin-N2-yl)-2-acetylaminofluorene (dG(N2)-AAF) lesion: a bulky adduct that persists in cellular DNA. *Chem. Res. Toxicol. 19*, 745−752.

(36) Leadon, S. A. T. R. M., and Cerutti, P. A. (1981) Excision repair of aflatoxin B1-DNA adducts in human fibroblasts. *Cancer Res. 41*, 5125−5129.

DOI: 10.1021/acs.chemrestox.6b00240
Chem. Res. Toxicol. XXXX, XXX, XXX−XXX

(37) Mao, H., Deng, Z., Wang, F., Harris, T. M., and Stone, M. P. (1998) An Intercalated and Thermally Stable FAPY Adduct of Aflatoxin B1 in a DNA Duplex: Structural Refinement from 1H NMR. *Biochemistry 37*, 4374−4387.
(38) Krzeminski, J. K., Kropachev, K., Reeves, D., Kolbanovskiy, A., Kolbanovkiy, M., Chen, K.-M., Sharma, A. K., Geacintov, N., Amin, S., and El-Bayoumy, K. (2013) Adenine-DNA adduct derived from the nitroreduction of 6-nitrochrysene is more resistant to nucleotide excision repair than guanine-DNA adducts. *Chem. Res. Toxicol. 26*, 1746−1754.
(39) Turesky, R. J., Markovic, J., and Aeschlimann, J.-M. (1996) Formation and differential removal of C-8 and N2-guanine adducts of the food carcinogen 2-amino-3-methylimidazo[4,5-f]quinoline in the liver, kidney, and colorectum of the rat. *Chem. Res. Toxicol. 9*, 397−402.
(40) Buterin, T. H., M, T., uneva, N., Geacintov, N. E., Amin, S., Kroth, H., Seidel, A., and Naegeli, H. (2000) Unrepaired fjord region polycyclic aromatic hydrocarbon-DNA adducts in ras Codon 61 mutational hot spots. *Cancer Res. 60*, 1849−1856.
(41) Kropachev, K. K. M., Liu, Z., Cai, Y., Zhang, L., Schwaid, A. G., Kolbanovskiy, A., Ding, S., Amin, S., Broyde, S., and Geacintov, N. E. (2013) Adenine-DNA adducts derived from the highly tumorigenic dibenzo[a,l]pyrene are resistant to nucleotide excision repair while guanine adducts are not. *Chem. Res. Toxicol. 26*, 783−793.
(42) Zhang, S.-M. C., Chen, K.-M., Sun, Y.-W., Aliaga, C., Lin, J.-M., Sharma, A. K., Amin, S., and El-Bayoumy, K. (2014) Simultaneous detection of deoxyadenosine and deoxyguanosine adducts in the tongue and other oral tissues of mice treated with dibenzo[a,l]pyrene. *Chem. Res. Toxicol. 27*, 1199−1206.
(43) Bieler, C. A., Cornelius, M. G., Stiborova, M., Arlt, V. M., Wiessler, M., Phillips, D. H., and Schmeiser, H. H. (2007) Formation and persistence of DNA adducts formed by the carcinogenic air pollutant 3-nitrobenzanthrone in target and non-target organs after intratracheal instillation in rats. *Carcinogenesis 28*, 1117−1121.
(44) Glatt, H., Pietsch, K. E., Sturla, S. J., and Meinl, W. (2014) Sulfotransferase-independent genotoxicity of illudin S and its acylfulvene derivatives in bacterial and mammalian cells. *Arch. Toxicol. 88*, 161.
(45) Stubbert, L. J., Smith, J. M., and McKay, B. C. (2010) Decreased transcription-coupled nucleotide excision repair capacity is associated with increased p53- and MLH1-independent apoptosis in response to cisplatin. *BMC Cancer 10*, 207.
(46) Hsu, P. H., Hanawalt, P. C., and Nouspikel, T. (2007) Nucleotide excision repair phenotype of human acute myeloid leukemia cell lines at various stages of differentiation. *Mutat. Res., Fundam. Mol. Mech. Mutagen. 614*, 3−15.
(47) Miyashita, H., Nakayama, K., Kanzaki, A., Takebayashi, Y., Ogura, O., Mori, S., Mutoh, M., Miyazaki, K., Fukumoto, M., and Pommier, Y. (2001) Loss of heterozygosity of nucleotide excision repair factors in sporadic ovarian, colon and lung carcinomas: implication for their roles of carcinogenesis in human solid tumors. *Oncol. Rep. 174*, 115−125.

DOI: 10.1021/acs.chemrestox.6b00240
Chem. Res. Toxicol. XXXX, XXX, XXX−XXX

Modulation of cytotoxicity by transcription-coupled nucleotide excision repair is independent of the requirement for bioactivation of acylfulvene

Claudia Otto,[a] Graciela Spivak,[b] Claudia Aloisi,[a] Mirco Menigatti,[c] Hanspeter Naegeli,[d] Philip C. Hanawalt,[b] Marina Tanasova,[a#] Shana J. Sturla[a]*

[a]Department of Health Science and Technology, ETH Zurich, 8092 Zurich, Switzerland.
[b]Department of Biology, Stanford University, Stanford CA 94305, United States
[c]Institute of Molecular Cancer Research, University of Zurich, Zurich 8057, Switzerland
[d]Institute of Pharmacology and Toxicology, University of Zurich-Vetsuisse, Zurich 8057, Switzerland

*Corresponding author: Department of Health Science and Technology, Institute of Food, Nutrition and Health, ETH Zurich, Schmelzbergstrasse 9, Zurich 8092, Switzerland
E-mail address: sturlas@ethz.ch (S. J. Sturla)
[#] Current address: Michigan Tech, Department of Chemistry, 620B Chem Sci Bldg., Houghton, MI 49931 USA
E-mail address: mtanasov@mtu.edu (M. Tanasova)

Table of Contents

Table S1. Gene sequences for real-time PCR analysis S3

Table S2. siRNA sequences S4

Figure S1. Relative PTGR1 level analysis by real-time RT-PCR S4

Figure S2. Silencing of NER factors XPC (A) and CSB (B) in SW480 and SW480-PTGR1 cells S5

Reverse-transcription real time PCR analysis of PTGR1 expression in WT and XP cells

Untreated WT and XP cells were collected from two flasks of 90-95% confluence as follows: 2 mL of 0.25% trypsin-EDTA was added and the cells were incubated for 5 min at 37 °C. Total mRNA was extracted from using the QIAGEN miRNeasy® mini kit and kept on dry ice until cDNA synthesis (Table S1). Synthesis of first-strand cDNA was performed with the Transcriptor First Strand cDNA Synthesis kit (Roche) according to manufacturer's instructions with random hexamer primers. Expression of prostaglandin reductase 1 (PTGR1, Gene ID: 22949) and of the reference gene porphobilinogen deaminase (PBGD, Gene ID: 3145) was measured with the LightCycler® 480 real-time PCR system and a LightCycler® 480 SYBR Green I master kit (Roche). The analysis was performed in duplicate and relative PTGR1 expression in the different cell lines was calculated by the method of Pfaffl et al.[26].

Table S1. Gene sequences for real-time PCR analysis[a]

Gene	Primer 5' → 3'	T, °C[b]	bp[c]
PTGR1	FW: GGCTCCTGAGCTTCAGGATG RV: GCTTCAAGCAGGACCTCTCCA	56	140
PBGD	FW: CAACGGCGGAAGAAAACAG RV: TCTCTCCAATCTTAGAGAGTG	56	195

[a]PTGR1, prostaglandin reductase, PBGD, porphobilinogen deaminase;
[b]annealing temperature; [c]product length, base-pairs (bp); FW, forward; RV, reverse.

The obtained data was normalized with respect to WT cells and is summarized in Figure S1.

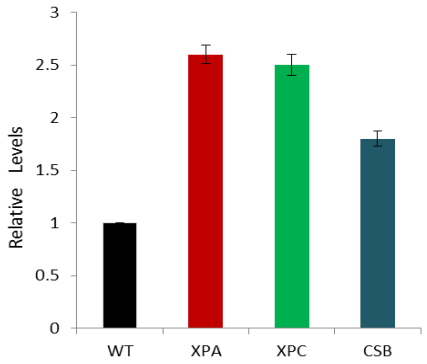

Figure S1. Relative PTGR1 levels established by correlating expression of the PTGR1-coding mRNA in a real-time reverse-transcription PCR analysis. The data is normalized to WT.

Knock down of NER factors in SW480 control and PTGR1 overexpressing cells and treatment with Acylfulvene

The siRNA sequences were purchased from Microsynth. Transfections were performed with Lipofectamine RNAiMAX according to the manufacturer's protocol (Invitrogen). The siRNA concentrations were 10 nM for non-coding siRNA and the silencing of XPC and CSB targets (siRNA sequences are listed in Supplementary Material). Cells were analyzed 72 h after siRNA transfections by Western blot. For treatment with Acylfulvene, cells were seeded 48 h after siRNA transfection in 96-well plates at a density of 3.0 $\times 10^3$ cells/well and were allowed to attach overnight. Cell viability experiments were initiated by replacing the maintenance media with media containing AF (0, 10, 100, 150, 300, 500, 1000, and 5000 nM final concentration, 0.1-0.5 % DMSO). Cell viability was measured 48 h later with the CellTiter-Glo® Luminescent Cell Viability Assay according to the manufacturer's protocol (Promega). This assay determines the number of viable cells in culture based on quantitation of the present ATP as an indicator of metabolically active cells.

Table S2. siRNA sequences

Target	Sequence 5' -> 3'	Source / Reference
Non-coding	AAU UCU CCG AAC GUG UCA CGU	Qiagen, Cat. No. SI03650325
XPC	GCA AAU GGC UUC UAU CGA ATT	Qiagen, Cat. No. SI00066227
CSB	GAA GCA AGG UUG UAA UAA ATT	Microsynth

XPC and CSB levels in SW480 control and SW480 PTGR1 cells after siRNA treatment

Cells were collected after 72 hours of siRNA treatment and lysed in RIPA buffer (Pierce, Thermo Scientific) containing protease inhibitors (Complete Tablets EDTA-free EASYpack, Roche). After cell lysis 40 µg protein of each sample were loaded onto an SDS PAGE gel (4-12 % NuPAGE bis-tris gels, Invitrogen), electrophoresed at 200V for 180min in 1x MOPS running buffer (NuPAGE MOPS SDS Running buffer 20x, Life Technologies) and transferred onto PVDF membranes (Amersham Hybond-P) at 30V for 50min. Staining of NER factors was performed with the following primary antibodies and respective secondary HRP antibodies: Mouse-anti-XPC (Abcam, 1:500), and rabbit-anti-CSB (Abcam, 1:500). All primary antibodies were diluted in 3 % BSA, TBS-Tween. Western blots were developed with Pierce ECL western blotting substrate (Thermo Scientific) and exposure to X-ray film.

Fig. S2. Silencing of NER factors XPC (A) and CSB (B) in SW480 and SW480-PTGR1 cells. M: Marker; siNC: siRNA with non-coding sequence, siXPC: siRNA targeting XPC, siCSB: siRNA targeting CSB. GAPDH served as loading control.